

# Multi-scale simulation of capillary pores and gel pores in Portland cement paste

Peng Gao<sup>1,2,3\*</sup>, Guang Ye<sup>3,4</sup>, Jiangxiong Wei<sup>1,2</sup>, Qijun Yu<sup>1,2</sup>

1. School of Materials Science and Engineering, South China University of Technology, Guangzhou 510640, People's Republic of China
2. Guangdong Low Carbon Technologies Engineering Center for Building Materials, South China University of Technology, Guangzhou 510640, People's Republic of China
3. Microlab, Faculty of Civil Engineering and Geosciences, Delft University of Technology, Delft, 2628 CN, The Netherlands
4. Magnel Lab for Concrete Research, Department of Structural Engineering, Ghent University, Ghent 9052, Belgium

## Abstract

The microstructures of Portland cement paste (water to cement ratio is 0.4, curing time is from 1 day to 28 days) are simulated based on the numerical cement hydration model, HUMOSTRUC3D (van Breugel, 1991; Koenders, 1997; Ye, 2003). The nanostructures of inner and outer C-S-H are simulated by the packing of mono-sized (5 nm) spheres. The pore structures (capillary pores and gel pores) of Portland cement paste are established by upgrading the simulated nanostructures of C-S-H to the simulated microstructures of Portland cement paste. The pore size distribution of Portland cement paste is simulated by using the image segmentation method (Shapiro and Stockman, 2001) to analyse the simulated pore structures of Portland cement paste. The simulation results indicate that the pore size distribution of the simulated capillary pores of Portland cement paste at the age of 1 day to 28 days is in a good agreement with the pore size distribution determined by scanning electron microscopy (SEM). The pore size distribution of the simulated gel pores of Portland cement paste (interlayer gel pores of outer C-S-H and gel pores of inner C-S-H are not included) is validated by the pore size distribution obtained by mercury intrusion porosimetry (MIP). The pores with pore size of 20 nm to 100 nm occupy very small volume fraction in the simulated Portland cement paste at each curing time (0.69% to 1.38%). This is consistent with the experimental results obtained by nuclear magnetic resonance (NMR).

## Originality

- The numerical simulation of the pore structures of cement paste both including capillary pores and gel pores was merely reported. Both the capillary and gel pores of Portland cement paste are simulated in this study. The pore size distributions of the simulated gel pores and capillary pores of Portland cement paste are validated by the experiments determined by SEM, MIP and NMR.
- Both the simulation results and the experimental results obtained by NMR indicate that the pores with pore size of 20 nm to 100 nm occupy very few volume fraction in the Portland cement paste (less than 1.38%). The volume fraction of the pores with size of 20 nm to 100 nm determined by MIP method reaches approximate 10%. If the simulation results are reasonable, the pore size distribution obtained by MIP is inappropriate. It should be emphasized that MIP is very frequently used to determine the pore structures of cementitious materials, which provides us an inappropriate information on the pore structure of cement paste. From this view point, this study provides us a new understanding of the pore structure of cement paste.

**Keywords:** capillary pores; gel pores; simulation; SEM; cement paste; HUMOSTRUC3D; random close packing

---

\* Corresponding author: [p.gao@tudelft.nl](mailto:p.gao@tudelft.nl), Tel +31 (0)15-278 4001, Fax +31 (0)15-278 4001

## 1. Introduction

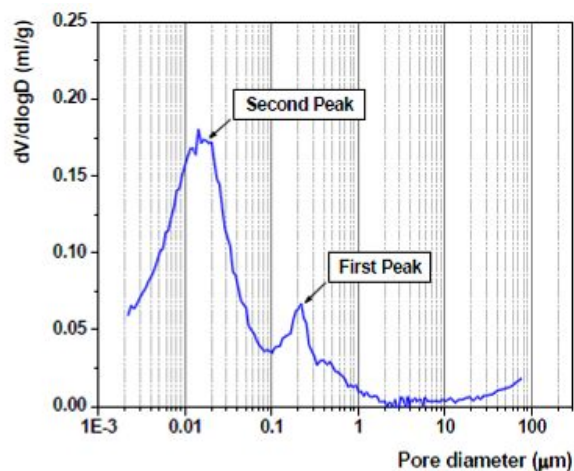
Cement paste is a multi-scale porous media with a large number of pores that ranges from nanometres to micrometres. The pore structures of cement paste, which mainly consists of gel pores and capillary pores, influence some performance of cement-based materials *e.g.* compressive strength, permeability, and durability. Capillary pores are considered as the remnants of the initially water-filled space (Taylor, 1997). Gel pores are an intrinsic part of C-S-H (Jennings, 2004). The pore structures of cement pastes can be described by several aspects: total porosity, connectivity of pore network and pore size distribution, *etc.* Total porosity and pore size distribution can be determined by scanning electron microscopy (SEM), mercury intrusion porosimetry (MIP), nuclear magnetic resonance (NMR), *etc.*

The diameters of capillary pores and gel pores are different. There are mainly two definitions:

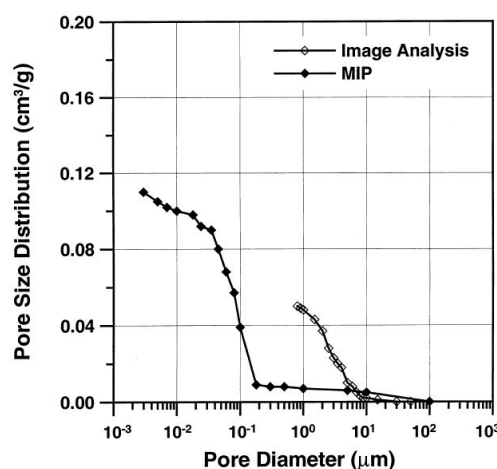
(1) Mindess, *et al.* (2003) summarized that capillary pores are larger than 10 nm and gel pores are smaller than 10 nm (Table 1). They probably gave this definition based on the experiments determined by MIP. From Figure 1 (Ye, 2003), two peaks exist in the typical pore size distribution curve determined by MIP. The first peak is larger than 10 nm, and considered as capillary pores. The second peak is smaller than 10 nm, and considered as gel pores.

Table 1 Classification of pore sizes in hydrated cement pastes (Mindess, *et al.*, 2003)

Designation	New pore category	Size of pore within structure
Capillary Pores	10-0.05 $\mu\text{m}$	Large capillaries (macropores)
	50-10 nm	Medium capillaries (large mesopores)
Gel Pores	10-2.5 nm	Small isolated capillaries (Small mesopores)
	2.5-0.5 nm	Micropores
	$\leq 0.5$ nm	Interlayer spaces



(a) MIP data from Ye (2003)



(b) MIP and SEM data presented by Diamond (2000)

Figure 1 Typical pore size distribution of cement paste determined by MIP and SEM

Diamond (2000) indicated that MIP is an inappropriate method to determine the pore size distribution of cement-based materials due to the effect of “ink-bottle” pores. In MIP testing, each pore size is assumed to correspond a minimum intrusion pressure of mercury. The pore size can be calculated based on the minimum intrusion pressure of mercury. In this calculation, the effect of “ink-bottle” pores causes errors. The “ink-bottle” pores means the pore system in which the large pore is not directly connected with outside (Diamond, 2000). The large pore in the “ink-bottle” pore is penetrated by mercury only when the pressure reaches a higher pressure. Because a lot of “ink-bottle” pores locate in the inside of cement-based materials, the effect of “ink-bottle” pores significantly reduces the accuracy of MIP for determining the large pores. Nevertheless, the pores smaller than a diameter (“threshold diameter”) can be accurately determined by MIP (Pichler, *et al.*, 2007). The “threshold

diameter” means that the pores of which diameter is greater than this diameter can form non connected path throughout the sample (Cui and Cahyadi, 2001; Ye, 2003). According to the experimental data presented in (Diamond, 2000), the threshold diameter ranges from 0.02  $\mu\text{m}$  to 0.3  $\mu\text{m}$ , which depends on water to cement (W/C) ratios and curing ages, etc. In comparison with the volume fraction of the pores determined by SEM, the volume fraction of the pores determined by MIP, are significantly lower (Figure 1b). Because the pore size distribution of capillary pores determined by MIP probably was incorrect, the classification of pore sizes in hydrated cement pastes shown in Table 1 might be inappropriate.

(2) According to the data of drying shrinkage versus weight loss (Figure 2), and Kelvin equation Jennings (2004) concluded that capillary pores are around 75 nm, and gel pores are smaller than 5 nm (Table 2).

Table 2 Characteristics of pores in cement paste (Jennings, 2004) Note: drying temperature was 60 °C

Pore category	New pore category	Size of pore within structure	RH Pores Empty % by Kelvin	Reversible Shrinkage Mechanism
Capillary	Capillary	75 nm	90	Capillary tension
Large Mesopores	Gel Inter low density (LD) C-S-H	2-5 nm	40	Disjoning
Small gel	Inter-globule	1.2-2 nm	20	Gibbs Bangham
Inter layer	Intra-globule or globule	<5 nm	0	Interlayer

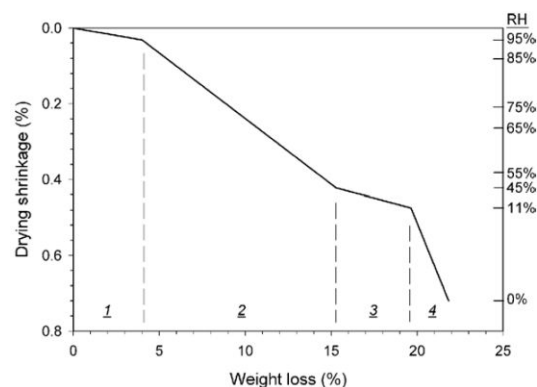


Figure 2 Sharp changes in slope at specific relative humidities (data taken from Roper, 1966, and drying temperature was 60 °C). The four regions shown here are suggestive of different drying rates exhibited by colloids (Jennings, 2004)

Based on the definition given by Jennings (2004), a multi-scale model is proposed to illustrate the pore structures of Portland cement paste:

(1) In the microscale (100 nm to 100  $\mu\text{m}$ ), capillary pores form in the outside space of cement grains (Figure 3a). In this scale, inner C-S-H and outer C-S-H has a “self-similar” structure, respectively (see Figure 3b).

(2) In the nanoscale (5 nm to 100 nm), as presented in Figure 3b, both the “self-similar” structures are generated by the packing of C-S-H globules. The packing density of inner C-S-H globules is higher than that of outer C-S-H globules. The gel pores form in the outside space of C-S-H globules.

(3) In the nanoscale (<5 nm), a C-S-H globule contains the layers of C-S-H chain and the interlayer water (Figure 3c). The gel pores inside C-S-H globules are called interlayer gel pores. (See the concept of C-S-H globules in the reports by Jennings, 2000, 2004, 2008).

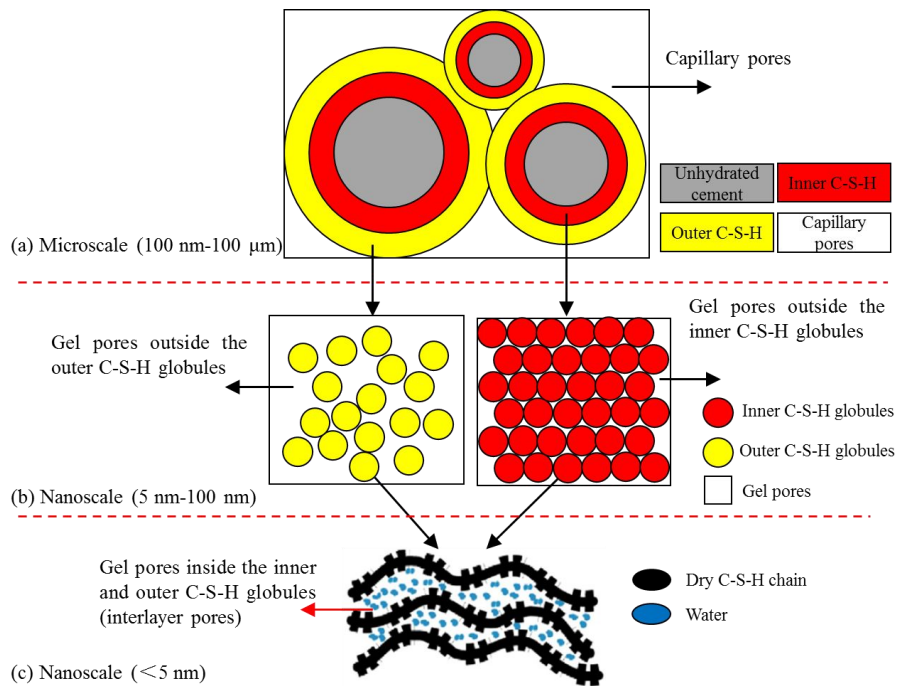


Figure 3 Schematic diagram of the multi-scale pore structures of cement paste  
 Note: The inner and outer C-S-H globules are assumed as the same. The concept of C-S-H globule was proposed by Jennings (2008)

In microscale (Figure 3a), some numerical cement hydration models *e.g.* HYMOSTRUC3D (van Breugel, 1991; Koenders, 1997 and Ye, 2003), CEMHYD3D (Bentz, 2005), and  $\mu\text{ic}$  microstructural modelling platform (Bishnoi and Scrivener, 2009) can be used to simulate the microstructures of cement paste. Based on the simulated microstructures, the capillary pore structures can be obtained (Ye, 2003). The gel pore structures, however, cannot be obtained from microstructure model. Ma and Li (2013) attempted to simulate the gel pore structures of cement paste by adding gel pores in C-S-H, but the detailed information was absent.

In nanoscale (Figure 3b), Bentz, *et al.* (1995), Fonseca and Jennings (2011), and Masoero, *et al.* (2012) numerically simulated the nanostructures of C-S-H by using the packing of spherical particles. Bentz, *et al.* (1995) used the hard core and soft shell model. Fonseca and Jennings (2011) used the random close packing, and the close packing of mono-sized spheres for simulating the nanostructures of outer C-S-H and inner C-S-H, respectively. Masoero, *et al.* (2012) employed the random close packing of multi-sized spheres for simulating the nanostructures of C-S-H. Both Fonseca and Jennings (2011), and Masoero *et al.* (2012) used the concept of C-S-H globules that was proposed by Jennings (2000, 2004, 2008). Evidently, if the nanostructures of C-S-H are simulated, the gel pore structures of C-S-H can be established. However, the detailed information on the gel pore size distribution of gel pores was not given.

Up to now, the numerical simulation of the pore structures of cement paste for both capillary pores and gel pores was merely reported. This study aims to develop a multi-scale approach to simulate the capillary pores of Portland cement paste in microscale (Figure 3a) and the gel pores outside the C-S-H globules in nanoscale (Figure 3b). Extended HYMOSTRUC3D is used to simulate the capillary pores of Portland cement paste, and the packing of spherical particles is used to simulate the gel pores outside the C-S-H globules. The gel pores of Portland cement paste are calculated based on the simulated microstructure of Portland cement paste and the simulated gel pores outside the C-S-H globules. In order to obtain the pore size distribution, the image segmentation method (Shapiro and Stockman, 2001) was employed to analyse the simulated pore structures (capillary pores and gel pores) of Portland cement paste. The simulated pore size distribution of Portland cement paste is validated by the experimental results of SEM (Ye, 2003), MIP (Ye, 2003) and NMR (Muller, 2014).

## 2. Multi-scale modelling approach

### 2.1 Microstructure of Portland cement paste

Extended HYMOSTRUC3D is used to simulate the hydration of Portland cement and the microstructures of Portland cement paste. The mineral composition of Portland cement is taken from Ye (2003) and Wang (2013): C3S (62.0%), C2S (10.5%), C3A (7.3%), C4AF (10.2%). The particle size distribution of Portland cement (Figure 4) and the W/C of Portland cement paste (0.4) are taken from Wang (2013). The hydration parameters of HYMOSTRUC3D ( $k_0$  and  $\delta_{tr}$ ) are calculated based on the mineral composition of Portland cement, respectively (Tuan, 2011). The calibration parameters of HYMOSTRUC3D ( $\beta_1$  and  $\beta_2$ ) are set as 1.0.

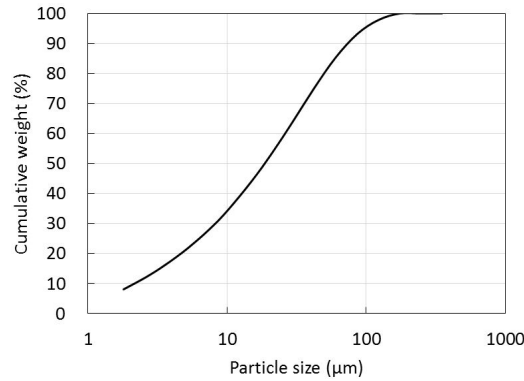


Figure 4 Particle size distribution of Portland cement (Wang, 2013)

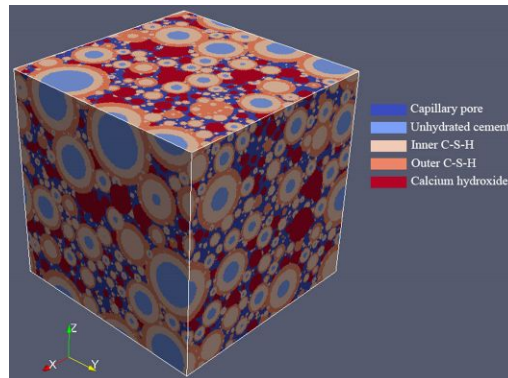


Figure 5 Simulated microstructure of Portland cement paste by extended HYMOSTRUC3D ( $100 \times 100 \times 100 \mu\text{m}^3$ , W/C=0.4, 28 days)

### 2.2 Nanostructures of C-S-H

The packing of mono-sized spheres is often used to understand the structures of various types of materials, *e.g.* liquids, granular media, glasses, and amorphous solids (Torquato, *et al.*, 2000). Different types of materials have different packing densities. For example, with increasing the packing density, the material should be liquid, jammed structures (amorphous solid), and crystal, respectively (Figure 6).

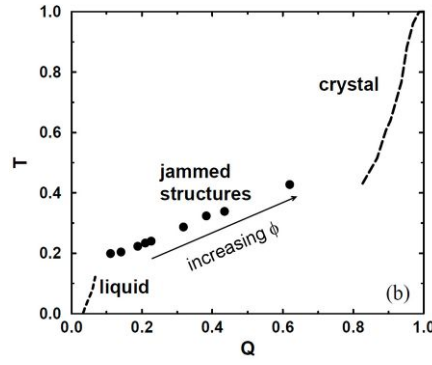


Figure 6 Molecular dynamics simulation results for the hard-sphere system (Torquato, *et al.*, 2000)

Note: T and Q are translational and orientational order parameters, respectively (see detailed information in the report by Torquato, *et al.*, 2000).  $\phi$  is the packing density.

This study assumes that the nanostructures of both inner C-S-H and outer C-S-H are generated by the packing of mono-sized spherical C-S-H globules (Figure 3b). The structure of C-S-H globules is the same for both inner C-S-H and outer C-S-H (Figure 3c). The diameter of each C-S-H globules is fixed at 5 nm based on the data from Jennings (2008). The packing density of inner C-S-H are higher than that of outer C-S-H.

### 2.2.1 Nanostructure of outer C-S-H

The nanostructure of outer C-S-H is simulated by the random close packing of mono-sized (5 nm) C-S-H globules (Figure 7a). The random close packing means “the maximum density that a large, random collection of spheres can attain and this density is a universal quantity” (Torquato, *et al.*, 2000). The packing density of the random close packing of mono-sized particles is approximate 0.64, which is very close to the packing density of C-S-H globules reported by Jennings, *et al.* (2007).

Theoretically the packing density of C-S-H globules can be calculated:

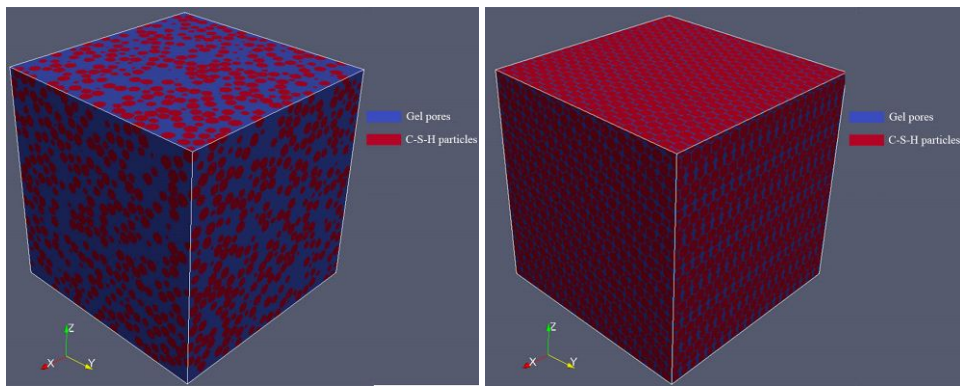
According to Jennings (2008), the density of C-S-H globule is  $2.604 \text{ g/cm}^3$ , and the chemical composition of C-S-H globule is  $\text{C}_{1.7}\text{SH}_{1.8}$ . From Lu *et al.* (1993), the chemical composition of outer C-S-H (outer C-S-H consists of both C-S-H globules and the water in the out space of C-S-H globules) is assumed to be  $\text{C}_{1.7}\text{SH}_4$  at 100% relative humidity. Thus, the water in the out space of C-S-H globules is 2.2 mol. The volume fraction of this water can be calculated:

$$V_{\text{Water}} = \frac{\frac{2.2 \times M_{\text{H}_2\text{O}}}{\rho_{\text{H}_2\text{O}}}}{\frac{2.2 \times M_{\text{H}_2\text{O}}}{\rho_{\text{H}_2\text{O}}} + \frac{M_{\text{C}_{1.7}\text{SH}_{1.8}}}{\rho_{\text{C}_{1.7}\text{SH}_{1.8}}}} \times 100\% \quad (1)$$

where  $M_{\text{H}_2\text{O}}$  (18 g/mol) is the mole weight of  $\text{H}_2\text{O}$ ,  $\rho_{\text{H}_2\text{O}}$  ( $1 \text{ g/cm}^3$ ) is the density of  $\text{H}_2\text{O}$ ,  $M_{\text{C}_{1.7}\text{SH}_{1.8}}$  (187.8 g/mol) is the mole weight of  $\text{C}_{1.7}\text{SH}_{1.8}$ ,  $\rho_{\text{C}_{1.7}\text{SH}_{1.8}}$  ( $2.604 \text{ g/cm}^3$ ) is the density of  $\text{C}_{1.7}\text{SH}_{1.8}$ .

Based on this equation, the volume fraction of the water in the outside space of C-S-H globules is equal to 35.4%. Theoretically the packing density of C-S-H globules in outer C-S-H is 64.6%, which confirms the packing density of outer C-S-H simulated by the random close packing of mono-sized (5 nm) C-S-H globules.

The random close packing has already been used to simulate the nanostructure of C-S-H gel (Fonseca, *et al.*, 2011; Masoero, *et al.*, 2012). In this study, the code from Skoge, *et al.* (2006) for the random close packing of mono-sized spheres is used to generate the nanostructure of outer C-S-H. The algorithm of this code is based on molecular dynamical mechanism. Because the diameter of C-S-H globules is assumed to be 5 nm, and the packing density of C-S-H globules is assumed to be 0.64, the input parameters of the code from Skoge, *et al.* (2006) are: the number of spheres is ten thousand, the max pressure is 200, and the max packing fraction is 0.65. Other input parameters are set at default (the events per sphere per cycle is 20, the initial packing density is 0.01, and the growth rate is 0.001).



(a) Simulated nanostructure of outer C-S-H (b) Simulated nanostructure of inner C-S-H

Figure 7 Simulated nanostructures of C-S-H

Note: Both the cubes are  $100 \times 100 \times 100 \text{ nm}^3$ . The packing density of outer C-S-H and inner C-S-H is about 0.64 and 0.74, respectively. In (a), ten thousand mono-sized spheres with a diameter of 5 nm are included.

### 2.2.2 Nanostructure of inner C-S-H

The nanostructure of inner C-S-H is simulated by the close packing of mono-sized (5 nm) C-S-H globules (Figure 7b). The close packing means the dense arrangement of mono-sized spheres in a lattice. The packing density of the close packing of mono-sized spheres is approximate 0.74 (Hales, 1998), which is higher than that of the random close packing.

### 2.3 Upscaling nanostructures of C-S-H to microstructures of Portland cement paste

In Figure 8a the representative volume of the microstructures of Portland cement paste is  $100 \times 100 \times 100 \mu\text{m}^3$ . It is digitalized into  $1000^3$  pixels, representing capillary pores, unhydrated cement, calcium hydroxide, outer C-S-H and inner C-S-H, respectively. The volume of each pixel is  $100 \times 100 \times 100 \text{ nm}^3$ . Both inner C-S-H pixels and outer C-S-H pixels have a “self-similar” nanostructures, respectively (Figure 8b). The simulated nanostructures of inner C-S-H and outer C-S-H are also digitalized into  $1000^3$  pixels, represent gel pores and C-S-H globules, respectively. C-S-H globules are considered as a solid phase. Based on the simulations the multiscale structures of Portland cement paste in microscale (Figure 8a) and nanoscale (Figure 8b) are generated.

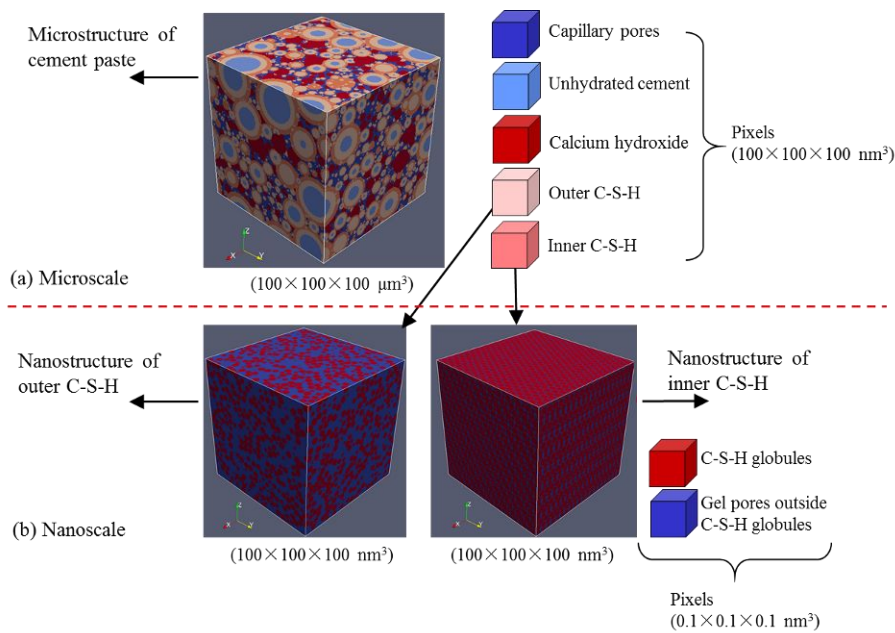


Figure 8 Multi-scale simulation of microstructures and nanostructures of Portland cement paste

## 2.4 Pore structures of Portland cement paste

The visual pore structures of Portland cement paste are obtained by removing the solid pixels in the microstructures and nanostructures. By removing the pixels of unhydrated cement, calcium hydroxide, outer C-S-H and inner C-S-H (Figure 8a), the capillary pores of cement paste are visualized (Figure 9a). By removing the pixels of C-S-H globules (Figure 8b), the gel pores of cement paste are visualized (Figure 9b).

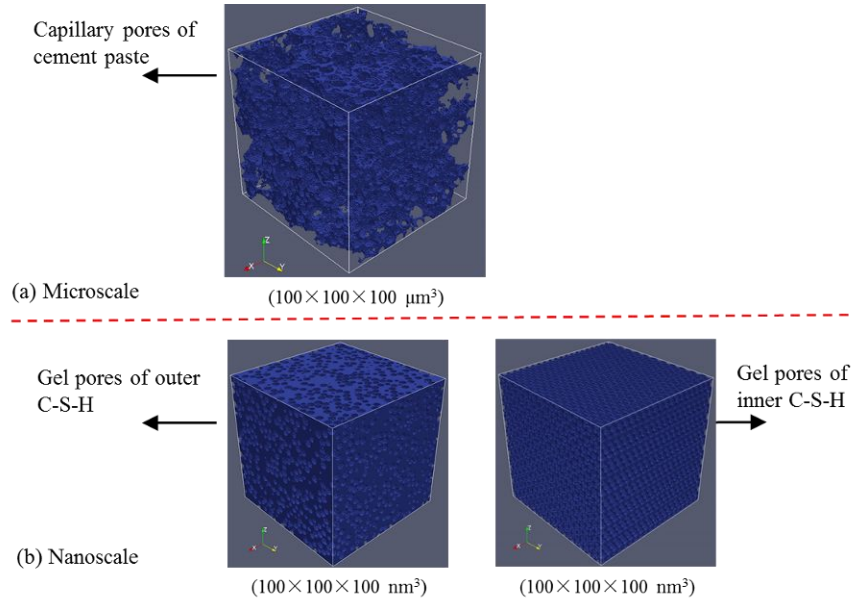


Figure 9 Simulated capillary pores and gel pores of Portland cement paste

Note: The interlayer gel pores are not simulated

## 2.5 Pore structures analysis

### 2.5.1 Image segmentation method

The image segmentation method (Shapiro and Stockman, 2001) is used to analyse the capillary pores and gel pores. The objects of the image segmentation method are the capillary pore structures of Portland cement paste (*e.g.* Figure 9a) and the gel pore structures of C-S-H (*e.g.* Figure 9b). For example, the microstructure of Portland cement paste (Figure 9a) is segmented into  $n$  slices. The thickness of each slice is equal to  $(100/n) \mu\text{m}$ . Then, each slice is digitalized into  $n \times n$  pixels. Like pore definition in SEM (Lange, *et al.*, 1994), a pore is defined as an area ( $A$ ) that contains the neighbour connected pixels of pores (blue pixels in Figure 10b).

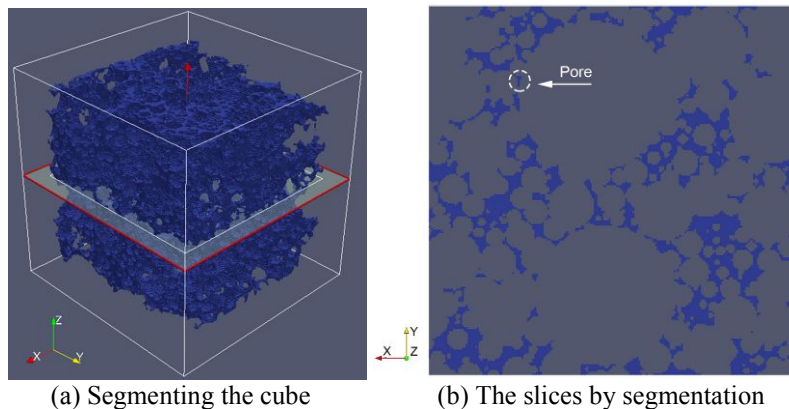


Figure 10 Schematic diagram of the image segmentation method



The virtual diameter of a pore area is defined. It is equal to  $(4A/\pi)^{0.5}$ . If the sum of the pore area with a diameter  $d$  on layer  $i$  is  $A_i$ , the volume of the pore area with a diameter  $d$  in the cube is:

$$V_d = \frac{100}{n} \times \sum_{i=1}^n A_i \quad (2)$$

where,  $V_d$  ( $\mu\text{m}^3$ ) is the total volume of the pore area with a diameter of  $d$  in the cube. If the objects of the image segmentation method are the simulated gel pore structures of C-S-H, the dimension of  $V_d$  should be  $\text{nm}^3$ .

### 2.5.2 Capillary pore size distribution

The image segmentation method to is employed to analyse the simulated microstructures of Portland cement paste. The volume fraction of capillary pores ( $V_{\text{d-capillary pore}}$ ) is calculated by Eq. (2). The number of slides  $n$  is set as 100, and the resolution or the distance between two adjacent slices is  $1 \mu\text{m}$ .

### 2.5.3 Gel pore size distribution

Both the cubes of the simulated nanostructures of inner C-S-H and outer C-S-H are analysed by the image segmentation method. The number of slides  $n$  is 100. The resolution of image segmentation is  $1 \text{ nm}$ . The gel pore size distribution of Portland cement paste is obtained by three steps:

- (1) The segmentation method is employed to analyse the simulated nanostructure of outer C-S-H, and the volume fraction of the gel pores of outer C-S-H ( $V_{\text{d-gel pore}}$ ) is calculated by Eq. (2).
- (2) The volume fraction of the outer C-S-H ( $f_{\text{Outer-C-S-H}}$ ) in the simulated microstructures ( $100 \times 100 \times 100 \mu\text{m}^3$ ) is calculated from the output data of HYMOSTRUC3D.
- (3) The volume fraction of gel pores in the Portland cement paste is equal to  $V_{\text{d-gel pore}} \times f_{\text{Outer-C-S-H}}$ . It should be emphasized that the interlayer gel pores cannot be determined by MIP, because the interlayer gel pores are smaller than  $1 \text{ nm}$  (Jennings, 2008). The gel pores outside inner C-S-H globules are inaccessible to nitrogen (Jennings and Tennis, 1994; Tennis and Jennings, 2000). Thus, gel pores outside inner C-S-H globules normally cannot be probed by MIP yet. In order to compare with experiments obtained by MIP, the interlayer gel pores and the gel pores outside inner C-S-H globules are excluded in the simulation of the gel pore size distribution.

## 3. Results and Discussion

### 3.1 Hydration and microstructures of Portland cement paste

The degree of hydration of Portland cement is shown in Figure 11. The simulated degree of hydration of Portland cement is validated with results determined by SEM (Ye G., 2003) and by Non-evaporable water method (Wang, 2013).

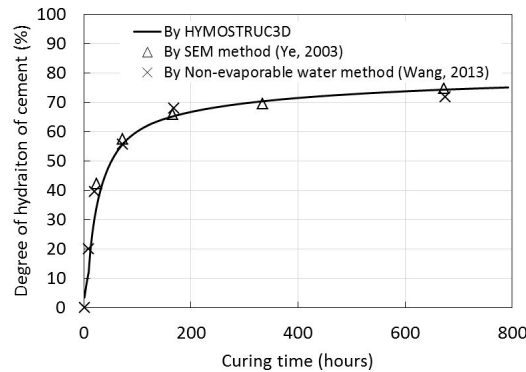


Figure 11 Degree of hydration of Portland cement (W/C=0.4)

The simulated microstructure of Portland cement paste at 28 days is indicated in Figure 5. The volume fractions of individual components including capillary pores, unhydrated cement, inner C-S-H, outer C-S-H and calcium hydroxide (CH) at different curing time up to 28 days are shown in Figure 12, respectively.

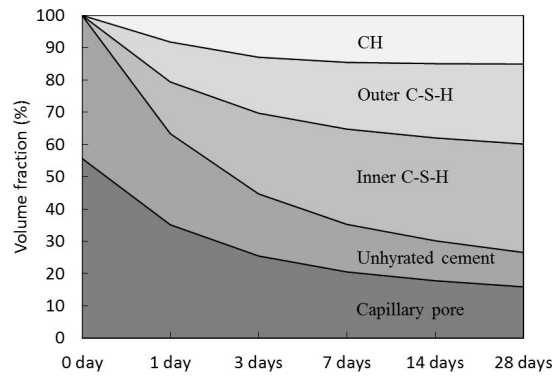


Figure 12 Volume fraction of individual component in the Portland cement paste.

### 3.2 Pore size distributions of simulated inner C-S-H and outer C-S-H

The pore size distributions of the simulated nanostructures of inner C-S-H and outer C-S-H are shown in Figure 13. The diameters of the gel pores of outer C-S-H are mainly smaller than 20 nm, and the diameters of the gel pores of inner C-S-H are mainly smaller than 4 nm.

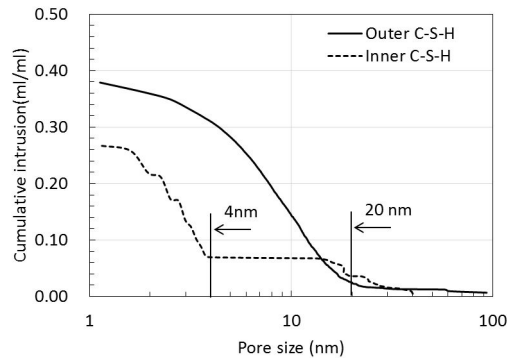


Figure 13 Gel pore size distributions of the simulated nanostructures of inner C-S-H and outer C-S-H

### 3.3 Pore structures of Portland cement paste

The pore size distributions (obtained by the image segmentation method) of the simulated capillary pores and gel pores of Portland cement paste are compared with the MIP and SEM data (Figure 14).

Based on the pore size distribution results shown in Figure 14, we found that:

(1) The simulated capillary pore structures of Portland cement paste can be validated by the SEM. From Figure 14, the simulated capillary pore size distribution of Portland cement paste from 1 day to 28 days are in good agreement with the SEM observations (Ye, 2003). The simulation results of this study is consistent with the simulation results of the capillary pores of Portland cement paste by Ye (2003).

(2) The volume of capillary pores ( $> 0.1$  nm) determined by MIP are much less than that determined by SEM and by simulation. However, the volume of gel pores ( $<$  threshold diameter) obtained by MIP are very close to that obtained from the simulation. As discussed, this is due to the effect of “ink-bottle” pores (Diamond, 2000; Pichler, *et al.*, 2007). According to the MIP data by Ye (2003), the threshold diameter of Portland cement paste in this study is set as 12.3 nm. From Figure 14, the pore size distribution results indicate that when the pore size is smaller than the threshold diameter, the gel pore size distribution of the simulated cement paste is very close to the gel pore size distribution of cement paste determined by MIP.

(3) The volume fraction of the pores with pore size of 20 nm to 100 nm of the simulated Portland cement paste is very small for each curing time (0.69% at 1 day, 0.97% at 3 days, 1.15% at 7 days, 1.28% at 14 days, 1.38% at 28 days). This is consistent with the results obtained by NMR (Figure 15), and the pore sizes of capillary pores and gel pores defined by Jennings (2004).

The multi-scale model of the pore structures of cement paste presented in Figure 3 could explain why the volume fraction of the pores with pore size from 20 nm to 100 nm in Portland cement paste is very small.

(1) In the multi-scale model of the pore structures of cement paste, the capillary pores form in microscale (Figure 3a). Thus, the capillary pores are mainly larger than 100 nm. This assumption is consistent with the observations by SEM (Figure 14).

(2) In the length scale of 5 nm to 100 nm (Figure 3b), the gel pores are generated by the packing of C-S-H globules. The gel pores are mainly in nanoscale and smaller than 100 nm. The diameter of gel pores depends on the packing density and the size of C-S-H globules. If the packing density of inner C-S-H and outer C-S-H is respectively fixed at 0.64 and 0.74, and the size of C-S-H globules is 5 nm, the gel pores of inner C-S-H and outer C-S-H are mainly smaller than 4 nm and 20 nm, respectively (Figure 13).

(3) In the length scale of < 5 nm (Figure 3c), the gel pores are the interlayer pores (Jennings, 2008). The diameters of the interlayer gel pores are less than 1 nm (Figure 15a).

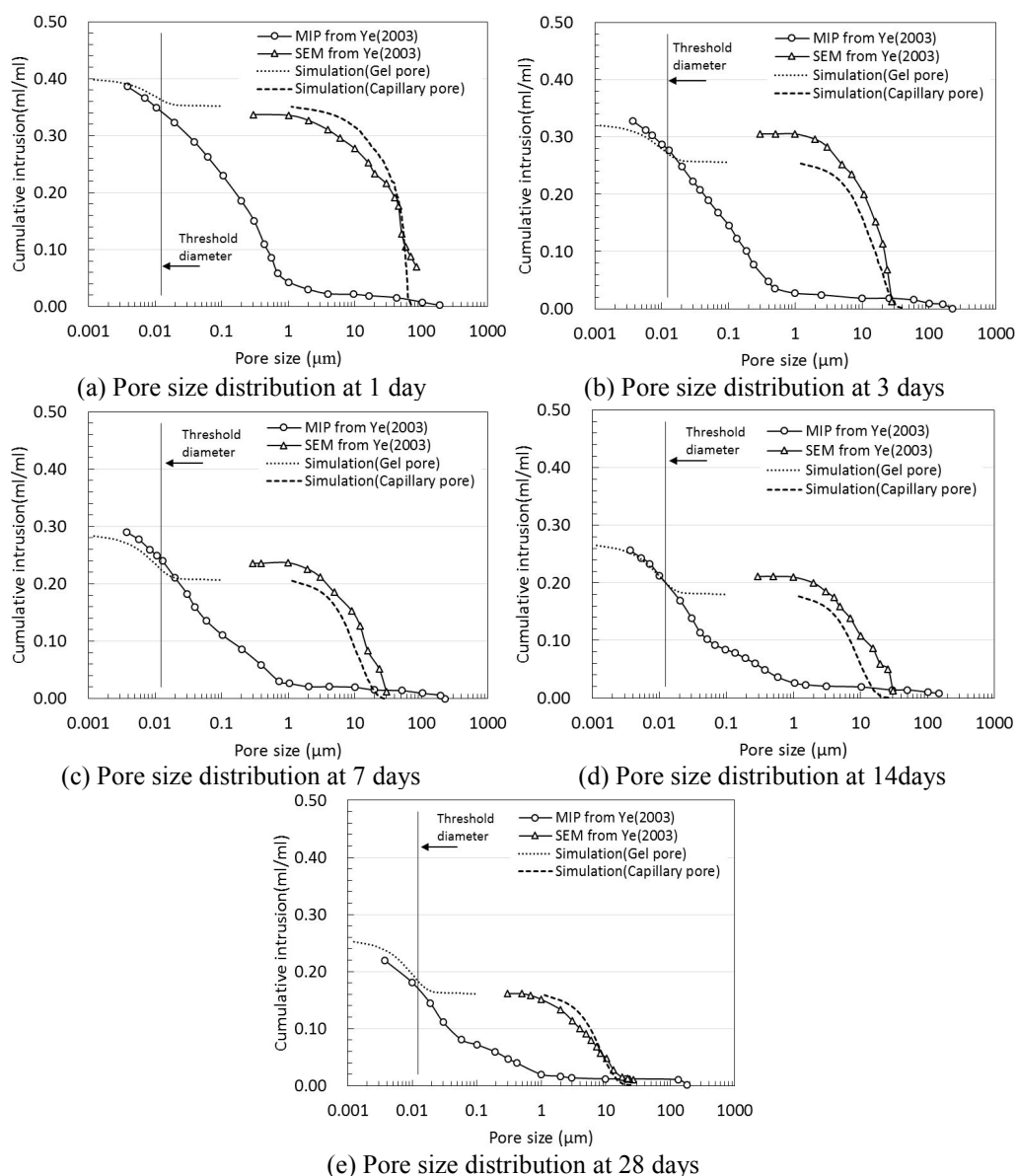


Figure 14 Pore size distribution of Portland cement paste at different curing time

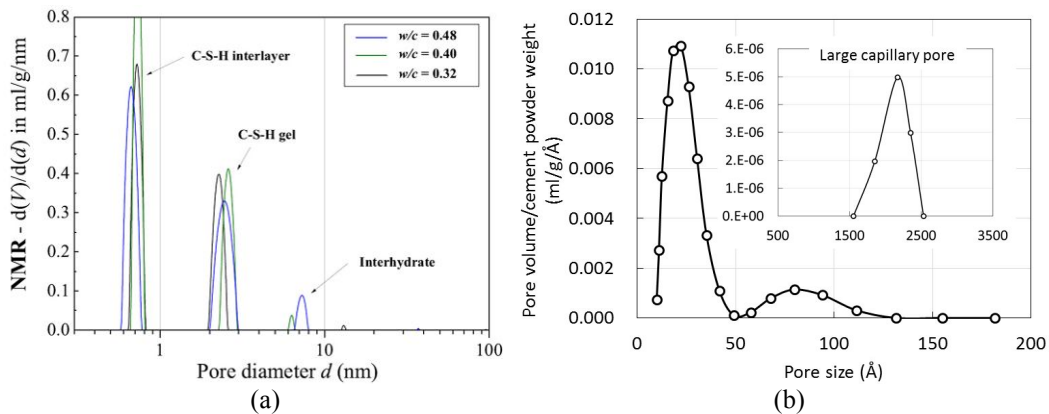


Figure 15 Pore size distributions of white cement paste determined by NMR  
 (a) White cement pastes with W/C = 0.48, 0.40, 0.32 at 28 days (Muller, 2014)  
 (b) White cement paste (W/C=0.43) at 122 days (modified from Jehng, *et al.*, 1996)

Based on above analysis, the capillary pores are mainly larger than 100 nm, and the gel pores are mainly smaller than 20 nm. As a consequence, the volume fraction of the 20 nm to 100 nm pores is very small in the Portland cement paste.

It should be kept in mind that the volume fraction of the 20 nm to 100 nm pores determined by MIP, in contrast, is much larger (10.4% at 1 day, 12.5% at 3 days, 12.6% at 7 days, 11.2% at 14 days, and 9.2% at 28 days). As mentioned in previous, MIP experiments have big errors on determining the pores larger than threshold diameters. MIP experiments provides us an inappropriate information on the pore structures of Portland cement paste, especially the pores with pore size of 20 nm to 100 nm.

Figure 16 is the supplemental material of Figure 14. As indicated in Figure 14, there is a “gap” or an absent information between the simulated gel pores and the simulated capillary pores. This is due to the influence of the resolution of image segmentation on the simulation of the capillary pore size distribution. The resolution determines the smallest pores presented in Figure 14. If the resolution of 0.1  $\mu\text{m}$  is used for the simulation of the capillary pore size distribution, the smallest capillary pore determined by the image segmentation method is around 0.113  $\mu\text{m}$ . According to Figure 16, the volume fraction of the pores smaller than 1  $\mu\text{m}$  which are determined by the image segmentation method with high resolutions such as 0.1  $\mu\text{m}$  and 0.2  $\mu\text{m}$  (the resolution of SEM in Ye, 2003 is 0.185  $\mu\text{m}$ ) are close to zero. It means that the resolution of image segmentation for the capillary pores simulation, in fact, does not significantly influence the results of capillary pores smaller than 1.0  $\mu\text{m}$ , if the capillary pores smaller than 1.0  $\mu\text{m}$  are assumed to be zero. This study uses the resolution of 1.0  $\mu\text{m}$  rather than others, because the capillary pore size distribution (larger than 1.0  $\mu\text{m}$ ) simulated by using the resolution of 1.0  $\mu\text{m}$  is more close to that determined by SEM.

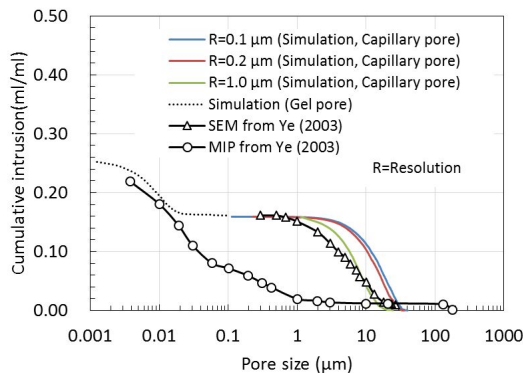


Figure 16 Influence of the resolution of image segmentation on the simulation of capillary pore size distribution

#### 4. Conclusions

(1) A multi-scale modelling approach has been proposed to simulate the microstructures of Portland cement paste ( $W/C=0.4$ ) and the nanostructures of inner and outer C-S-H. The pore structures of Portland cement paste including capillary pores and gel pores are modelled.

(2) The pore size distribution of the simulated capillary pores of Portland cement paste at the age from 1 day to 28 days is in a good agreement with the pore size distribution of capillary pores obtained by SEM. The pore size distribution of the simulated gel pores of Portland cement paste at the age of 1 day to 28 days is validated by the pore size distribution of gel pores obtained by MIP.

(3) The simulation results indicate that the pores with pore size of 20 nm to 100 nm occupy a very small volume fraction in the Portland cement paste at each curing time. This is consistent with the data obtained by NMR experiments.

### **Acknowledgements**

This work was funded by the China Scholarship Council (CSC), and the Research Centre of TU Delft in Urban System and Environment (No. C36103) and the National Basic Research Program of China (973 Program: 2011CB013800). The authors would like to thank Mr. Hua Dong for his advice in the numerical simulation.

### **References**

- Bentz D.P., 2005. CEMHYD3D: A Three-dimensional cement hydration and microstructure development modeling package. Version 3.0, NISTIR 7232, U.S. Department of Commerce, Available at, <http://concrete.nist.gov/monograph>.
- Bentz D.P., Quenard D.A., Baroghel-Bouny V., Garboczi E.J. and Jennings H.M., 1995. Modelling drying shrinkage of cement paste and mortar Part 1. Structural models from nanometres to millimetres. *Materials and Structures*, 28, 450-458.
- Bishnoi S. and Scrivener K.L., 2009.  $\mu$ c: A new platform for modelling the hydration of cements. *Cement and Concrete Research*, 39, 266-274.
- Cui L. and Cahyadi J.H., 2001. Permeability and pore structure of OPC paste. *Cement and Concrete Research*, 31, 277-282.
- Diamond S., 2000. Mercury porosimetry: An inappropriate method for the measurement of pore size distributions in cement-based materials. *Cement and Concrete Research*, 30, 1 517-1 525.
- Fonseca P.C., Jennings H.M. and Andrade J.E., 2011. A nanoscale numerical model of calcium silicate hydrate. *Mechanics of Materials*, 43, 408-419.
- Hales T. C., 1998. An overview of the Kepler conjecture. arXiv preprint math/9811071.
- Jehng J.Y., Sprague D.T. and Halperin W.P., 1996. Pore structure of hydrating cement paste by magnetic resonance relaxation analysis and freezing. *Magnetic Resonance Imaging*, 41, 785-791.
- Jennings H.M. and Tennis P.D., 1994. Model for the developing microstructure in Portland cement pastes. *Journal of American Ceramic Society*, 77, 3 161-3 172.
- Jennings H.M., 2000. A model for the microstructure of calcium silicate hydrate in cement paste. *Cement and Concrete Research*, 30, 101-116.
- Jennings H. M., 2004. Colloid model of C-S-H and implications to the problem of creep and shrinkage. *Materials and Structures*, 37, 59-70.
- Jennings H.M., 2008. Refinements to colloid model of C-S-H in cement: CM-II. *Cement and Concrete Research*, 38, 275-289.
- Jennings H.M., Thomas J.J., Gevrenov J.S., Constantinides G. and Ulm F.J., 2007. A multi-technique investigation of the nanoporosity of cement paste. *Cement and Concrete Research*, 37, 329-336.
- Koenders E.A.B., 1997. Simulation of volume changes in hardening cement-based materials. PhD Thesis, Delft, Delft University of Technology, The Netherlands.
- Lange D.A., Jennings H.M. and Shah S.P., 1994. Image analysis techniques for characterization of pore structure of cement-based materials. *Cement and Concrete Research*, 24, 841-853.
- Lu P., Sun G. and Young J.F., 1993. Phase Composition of Hydrated DSP Cement Pastes. *Journal of American Ceramic Society*, 76, 1 003-1 007
- Ma H.Y. and Li Z.J., 2013. Realistic pore structure of Portland cement paste: experimental study and numerical simulation. *Computers and Concrete*, 11, 317-336.
- Masoero E., Del Gado E., Pellenq R.J.-M., Ulm F.J. and Yip S., 2012. Nanostructure and nanomechanics of cement: Polydisperse colloidal packing. *Physical Review Letters*, 109, 155503.
- Mindess S., Young J.F. and Darwin D., 2003. Concrete. 2<sup>nd</sup> ed. Prentice-Hall, Englewood Cliffs.

- Muller A.C.A., 2014. Characterization of porosity & C-S-H in cement pastes by <sup>1</sup>H NMR. PhD Thesis, Lausanne, Swiss Federal Institute of Technology in Lausanne, Switzerland.
- Pichler C., Lackner R. and Mang H.A., 2007. A multiscale micromechanics model for the autogenous-shrinkage deformation of early-age cement-based materials. *Engineering Fracture Mechanics*, 74, 34-58.
- Roper H., 1966. Dimensional change and water sorption studies of cement paste. *Symposium on Structure of Portland Cement Paste and Concrete*, Washington, D.C.
- Shapiro L.G., and Stockman G.C., 2001. *Computer Vision*. 1<sup>st</sup> ed. Upper Saddle River, NJ: Prentice Hall.
- Skoge M. and Donev A., Stillinger F.H. and Torquato S., 2006. Packing hyperspheres in high-dimensional Euclidean spaces. *Physical Review E*, 74, 041127.
- Taylor H.F.W., 1997. *Cement Chemistry*. 2<sup>nd</sup> ed. London: Thomas Telford Publishing.
- Tennis P.D. and Jennings H.M., 2000. A model for two types of calcium silicate hydrate in the microstructure of Portland cement pastes. *Cement and Concrete Research*, 77, 3 161-3 172.
- Tuan N.V., 2011. Rice husk ash as a mineral admixture for ultra high performance concrete. PhD Thesis, Delft, Delft University of Technology, The Netherlands.
- Torquato S., Truskett T.M. and Debenedetti P.G., 2000. Is random close packing of spheres well defined? *Physical Review Letters*, 84, 2 064-2 067.
- van Breugel K., 1991. Simulation of hydration and formation of structure in hardening cement-based materials. PhD Thesis, Delft, Delft University of Technology, The Netherlands.
- Wang Y., 2013. Performance assessment of cement-based materials blended with micronized sand: microstructure, durability and sustainability. PhD Thesis, Delft, Delft University of Technology, The Netherlands.
- Ye G., 2003. Experimental Study and Numerical Simulation of the Development of the Microstructure and Permeability of Cementitious Materials. PhD Thesis, Delft, Delft University of Technology, The Netherlands.